

Hydration Isomers of Protonated Phenylalanine and Derivatives: Relative Stabilities from Infrared Photodissociation

James S. Prell, Terrence M. Chang, Jeremy T. O'Brien, and Evan R. Williams*

Department of Chemistry, University of California, Berkeley, California 94720

Received April 1, 2010; E-mail: williams@cchem.berkeley.edu

Abstract: The binding sites of water molecules to protonated Phe and its derivatives are investigated using infrared photodissociation (IRPD) spectroscopy and kinetics as well as by computational chemistry. Calculated relative energies for hydration of PheH^+ at various sites on the N- and C-termini depend on the type of theory and basis set used, and no one hydration site was consistently calculated to be most favorable. Infrared photodissociation (IRPD) spectra between ~ 2650 and 3850 cm^{-1} are reported for $\text{PheH}^+(\text{H}_2\text{O})_{1-4}$ at 133 K and compared to calculated absorption spectra of low-energy hydration isomers, which do not resemble the IRPD spectra closely enough to unambiguously assign spectral bands. The IRPD spectra of $\text{PheH}^+(\text{H}_2\text{O})_{1-4}$ are instead compared to those of $N,N\text{-Me}_2\text{PheH}^+(\text{H}_2\text{O})_{1,2}$, $N\text{-MePheH}^+(\text{H}_2\text{O})_{1-3}$, and $\text{PheOMeH}^+(\text{H}_2\text{O})_{1-3}$ at 133 K, which makes possible systematic band assignments. A unique band associated with a binding site not previously reported for $\text{PheH}^+(\text{H}_2\text{O})$, in which the water molecule accepts a hydrogen bond from the N-terminus of PheH^+ and donates a weak hydrogen bond to the π -system of the side chain, is identified in the IRPD spectra. IRPD kinetics at laser frequencies resonant with specific hydration isomers are found to be biexponential for $N,N\text{-Me}_2\text{PheH}^+(\text{H}_2\text{O})$, $N\text{-MePheH}^+(\text{H}_2\text{O})$, and $\text{PheH}^+(\text{H}_2\text{O})$. Relative populations of ions with water molecules attached at various binding sites are determined from fitting these kinetic data, and relative energies for hydration of these competitive binding sites at 133 K are obtained from these experimental values.

Introduction

Water plays a key role in the structure and function of biomolecules and is common in interfaces between molecules in macromolecular complexes. Insight into how water interacts with peptides and proteins, affects their dynamical motion, and stabilizes intra- and intermolecular interactions, such as salt bridges, can provide a better understanding of factors that contribute to protein structure and function. Water-protein interactions have been investigated in solution using a number of different techniques, such as NMR,¹⁻³ X-ray and neutron diffraction,⁴ and femtosecond spectroscopy.⁵ Rotation of water molecules in the first hydration shell of proteins can be $\sim 2-5$ times slower compared to bulk water molecules,^{2,6} and residence times of buried water molecules can be orders of magnitude longer than those at the protein surface.^{1,2,6} Specific water molecules are often observed in crystal structures, which can be a result of trapping or tight binding.⁷ Due to the large number

of interactions that cooperate or compete in water-protein binding, it can be difficult to determine the relative contributions of proximal functional groups and surrounding solvent molecules to observed hydration behavior.

Water interactions with a variety of biomolecules have also been investigated in the gas phase, where effects of individual functional groups on hydration can be more clearly distinguished and effects of the surrounding solvent can in principle be inferred by comparisons to condensed-phase results. Hydration equilibrium,⁸⁻¹² blackbody infrared radiative dissociation (BIRD),¹³⁻¹⁸ high pressure mass spectrometry,¹⁹⁻²⁵ and guided

- (1) Denisov, V. P.; Halle, B. *Faraday Discuss.* **1996**, *103*, 227-244.
- (2) Halle, B. *Philos. Trans. R. Soc. London, Ser. B* **2004**, *359*, 1207-1223.
- (3) Otting, G. *Prog. Nucl. Magn. Reson. Spectrosc.* **1997**, *31*, 259-285.
- (4) Svergun, D. I.; Richard, S.; Koch, M. H. J.; Sayers, Z.; Kuprin, S.; Zaccai, G. *Proc. Natl. Acad. Sci. U.S.A.* **1998**, *95*, 2267-2272.
- (5) Qiu, W. H.; Kao, Y. T.; Zhang, L. Y.; Yang, Y.; Wang, L. J.; Stites, W. E.; Zhong, D. P.; Zewail, A. H. *Proc. Natl. Acad. Sci. U.S.A.* **2006**, *103*, 13979-13984.
- (6) Makarov, V. A.; Andrews, B. K.; Smith, P. E.; Pettitt, B. M. *Biophys. J.* **2000**, *79*, 2966-2974.
- (7) Williams, M. A.; Goodfellow, J. M.; Thornton, J. M. *Protein Sci.* **1994**, *3*, 1224-1235.

- (8) Gao, B.; Wytttenbach, T.; Bowers, M. T. *J. Am. Chem. Soc.* **2009**, *131*, 4695-4701.
- (9) Gao, B.; Wytttenbach, T.; Bowers, M. T. *J. Phys. Chem. B* **2009**, *113*, 9995-10000.
- (10) Liu, D. F.; Wytttenbach, T.; Barran, P. E.; Bowers, M. T. *J. Am. Chem. Soc.* **2003**, *125*, 8458-8464.
- (11) Liu, D. F.; Wytttenbach, T.; Bowers, M. T. *Int. J. Mass Spectrom.* **2004**, *236*, 81-90.
- (12) Wytttenbach, T.; Bowers, M. T. *Chem. Phys. Lett.* **2009**, *480*, 1-16.
- (13) Lemoff, A. S.; Bush, M. F.; Williams, E. R. *J. Am. Chem. Soc.* **2003**, *125*, 13576-13584.
- (14) Lemoff, A. S.; Bush, M. F.; O'Brien, J. T.; Williams, E. R. *J. Phys. Chem. A* **2006**, *110*, 8433-8442.
- (15) Lemoff, A. S.; Wu, C. C.; Bush, M. F.; Williams, E. R. *J. Phys. Chem. A* **2006**, *110*, 3662-3669.
- (16) Lemoff, A. S.; Bush, M. F.; Wu, C. C.; Williams, E. R. *J. Am. Chem. Soc.* **2005**, *127*, 10276-10286.
- (17) Lemoff, A. S.; Williams, E. R. *J. Am. Soc. Mass Spectrom.* **2004**, *15*, 1014-1024.
- (18) Jockusch, R. A.; Lemoff, A. S.; Williams, E. R. *J. Phys. Chem. A* **2001**, *105*, 10929-10942.

ion beam experiments²⁶ have been used to measure enthalpies and/or entropies for hydration of metal cationized or protonated amino acids and peptides by a discrete number of water molecules. These studies reveal that the binding energy of the first water molecule to a protonated aliphatic or aromatic amino acid is ~14–19 kcal/mol, and binding energies of subsequent water molecules decrease to values near the vaporization enthalpy of water (10.5 kcal/mol).¹² For ions with only one low-energy hydration isomer, these values are direct measurements of the hydration thermodynamics of the associated hydration site. However, even for protonated amino acids, interpretation of sequential binding energies in terms of individual hydration sites can be more challenging. Computational chemistry indicates that neutral polar groups in these ions, such as carboxylic acid and hydroxyl groups, can compete with charge sites for hydration; thus it is often possible that multiple hydration isomers exist in a hydrated ion population, even for singly hydrated ions.^{9,27–29}

Infrared photodissociation (IRPD) spectroscopy is a powerful structural tool that has been used to elucidate detailed information about the structures of gas-phase organic ions and their hydrates,^{27,30–63} including ions for which more than one

structure is present.^{31,32,34,36,39,44,46,53,54,59–61,64} The hydrogen stretch region (~2500–3800 cm⁻¹) can be used to determine whether amino acids adopt a zwitterionic or nonzwitterionic form in such complexes^{30,32,33,46,62,63} as well as how water molecules hydrate ions.^{33,53,65–75} IRPD spectroscopy experiments show that the addition of a single water molecule to lithiated arginine induces a change from the nonzwitterionic to the zwitterionic form of the amino acid.³³ Results for hydrated, potassium tryptamine indicate that temperature can have a strong influence on ion hydration, and isomers calculated to be ~20 kJ/mol higher in energy than the lowest-energy structure were found to contribute substantially to the ~50–150 K IRPD spectrum of this ion, indicating kinetic trapping of high-energy structures or substantial uncertainties in calculated energies.⁷⁶

Pioneering IRPD spectroscopy studies by Rizzo and co-workers of ValH⁺(H₂O)_{1–4} are consistent with addition of the first three water molecules to the protonated N-terminus before the uncharged C-terminus is hydrated based on the presence of a spectral band associated with a bare carboxylic acid group.²⁷

- (19) Klassen, J. S.; Blades, A. T.; Kebarle, P. *J. Phys. Chem.* **1995**, *99*, 15509–15517.
- (20) Meot-Ner, M. *Chem. Rev.* **2005**, *105*, 213–284.
- (21) Meot-Ner, M.; Field, F. H. *J. Am. Chem. Soc.* **1974**, *96*, 3168–3171.
- (22) Wincel, H. *Int. J. Mass Spectrom.* **2006**, *251*, 23–31.
- (23) Wincel, H. *Chem. Phys. Lett.* **2007**, *439*, 157–161.
- (24) Wincel, H. *J. Phys. Chem. A* **2007**, *111*, 5784–5791.
- (25) Wincel, H. *J. Am. Soc. Mass Spectrom.* **2007**, *18*, 2083–2089.
- (26) Ye, S. J.; Moision, R. M.; Armentrout, P. B. *Int. J. Mass Spectrom.* **2006**, *253*, 288–304.
- (27) Kamariotis, A.; Boyarkin, O. V.; Mercier, S. R.; Beck, R. D.; Bush, M. F.; Williams, E. R.; Rizzo, T. R. *J. Am. Chem. Soc.* **2006**, *128*, 905–916.
- (28) Michaux, C.; Wouters, J.; Jacquemin, D.; Perpete, E. A. *Chem. Phys. Lett.* **2007**, *445*, 57–61.
- (29) Rozman, M. *J. Am. Soc. Mass Spectrom.* **2005**, *16*, 1846–1852.
- (30) Atkins, C. G.; Rajabi, K.; Gillis, E. A. L.; Fridgen, T. D. *J. Phys. Chem. A* **2008**, *112*, 10220–10225.
- (31) Armentrout, P. B.; Rodgers, M. T.; Oomens, J.; Steill, J. D. *J. Phys. Chem. A* **2008**, *112*, 2248–2257.
- (32) Bush, M. F.; O'Brien, J. T.; Prell, J. S.; Saykally, R. J.; Williams, E. R. *J. Am. Chem. Soc.* **2007**, *129*, 1612–1622.
- (33) Bush, M. F.; Prell, J. S.; Saykally, R. J.; Williams, E. R. *J. Am. Chem. Soc.* **2007**, *129*, 13544–13553.
- (34) Chen, X.; Yu, L.; Steill, J. D.; Oomens, J.; Polfer, N. C. *J. Am. Chem. Soc.* **2009**, *131*, 18272–18282.
- (35) Drayss, M. K.; Blunk, D.; Oomens, J.; Schäfer, M. *J. Phys. Chem. A* **2008**, *112*, 11972–11974.
- (36) Dunbar, R. C.; Hopkinson, A. C.; Oomens, J.; Siu, C. K.; Siu, K. W. M.; Steill, J. D.; Verkerk, U. H.; Zhao, J. F. *J. Phys. Chem. B* **2009**, *113*, 10403–10408.
- (37) Dunbar, R. C.; Steill, J. D.; Polfer, N. C.; Oomens, J. *J. Phys. Chem. B* **2009**, *113*, 10552–10554.
- (38) Eyler, J. R. *Mass Spectrom. Rev.* **2009**, *28*, 448–467.
- (39) Forbes, M. W.; Bush, M. F.; Polfer, N. C.; Oomens, J.; Dunbar, R. C.; Williams, E. R.; Jockusch, R. A. *J. Phys. Chem. A* **2007**, *111*, 11759–11770.
- (40) Fridgen, T. D.; MacAleese, L.; McMahon, T. B.; Lemaire, J.; Maitre, P. *J. Phys. Chem. Chem. Phys.* **2006**, *8*, 955–966.
- (41) Fujihara, A.; Matsumoto, H.; Shibata, Y.; Ishikawa, H.; Fuke, K. *J. Phys. Chem. A* **2008**, *112*, 1457–1463.
- (42) Gardenier, G. H.; Roscioli, J. R.; Johnson, M. A. *J. Phys. Chem. A* **2008**, *112*, 12022–12026.
- (43) Grégoire, G.; Gaigeot, M. P.; Marinica, D. C.; Lemaire, J.; Schermann, J. P.; Desfrancois, C. *J. Phys. Chem. Chem. Phys.* **2007**, *9*, 3082–3097.
- (44) Heaton, A. L.; Bowman, V. N.; Oomens, J.; Steill, J. D.; Armentrout, P. B. *J. Phys. Chem. A* **2009**, *113*, 5519–5530.
- (45) Kapota, C.; Lemaire, J.; Maitre, P.; Ohanessian, G. *J. Am. Chem. Soc.* **2004**, *126*, 1836–1842.
- (46) O'Brien, J. T.; Prell, J. S.; Steill, J. D.; Oomens, J.; Williams, E. R. *J. Am. Chem. Soc.* **2009**, *131*, 3905–3912.
- (47) Oh, H. B.; Lin, C.; Hwang, H. Y.; Zhai, H. L.; Breuker, K.; Zabrouskov, V.; Carpenter, B. K.; McLafferty, F. W. *J. Am. Chem. Soc.* **2005**, *127*, 4076–4083.
- (48) Oomens, J.; Steill, J. D. *J. Phys. Chem. A* **2008**, *112*, 3281–3283.
- (49) Polfer, N. C.; Oomens, J. *Mass Spectrom. Rev.* **2009**, *28*, 468–494.
- (50) Polfer, N. C.; Paizs, B.; Snoek, L. C.; Compagnon, I.; Suhai, S.; Meijer, G.; von Helden, G.; Oomens, J. *J. Am. Chem. Soc.* **2005**, *127*, 8571–8579.
- (51) Prell, J. S.; Flick, T. G.; Oomens, J.; Berden, G.; Williams, E. R. *J. Phys. Chem. A* 2009.
- (52) Prell, J. S.; O'Brien, J. T.; Steill, J. D.; Oomens, J.; Williams, E. R. *J. Am. Chem. Soc.* **2009**, *131*, 11442–11449.
- (53) Prell, J. S.; Williams, E. R. *J. Am. Chem. Soc.* **2009**, *131*, 4110–4119.
- (54) Prell, J. S.; Demireva, M.; Williams, E. R. *J. Am. Chem. Soc.* **2009**, *131*, 1232–1242.
- (55) Rajabi, K.; Fridgen, T. D. *J. Phys. Chem. A* **2008**, *112*, 23–30.
- (56) Rodgers, M. T.; Armentrout, P. B.; Oomens, J.; Steill, J. D. *J. Phys. Chem. A* **2008**, *112*, 2258–2267.
- (57) Simon, A.; MacAleese, L.; Maitre, P.; Lemaire, J.; McMahon, T. B. *J. Am. Chem. Soc.* **2007**, *129*, 2829–2840.
- (58) Stearns, J. A.; Boyarkin, O. V.; Rizzo, T. R. *J. Am. Chem. Soc.* **2007**, *129*, 13820–13821.
- (59) Stearns, J. A.; Mercier, S.; Seaiby, C.; Guidi, M.; Boyarkin, O. V.; Rizzo, T. R. *J. Am. Chem. Soc.* **2007**, *129*, 11814–11820.
- (60) Steill, J. D.; Oomens, J. *J. Am. Chem. Soc.* **2009**, *131*, 13570–13571.
- (61) Vaden, T. D.; de Boer, T. S. J. A.; Simons, J. P.; Snoek, L. C.; Suhai, S.; Paizs, B. *J. Phys. Chem. A* **2008**, *112*, 4608–4616.
- (62) Wu, R.; McMahon, T. B. *J. Mass Spectrom.* **2008**, *130*, 1641–1648.
- (63) Wu, R. H.; McMahon, T. B. *J. Am. Chem. Soc.* **2007**, *129*, 4864–4865.
- (64) Stearns, J. A.; Guidi, M.; Boyarkin, O. V.; Rizzo, T. R. *J. Chem. Phys.* **2007**, *127*, 154322.
- (65) Shin, J. W.; Hammer, N. I.; Diken, E. G.; Johnson, M. A.; Walters, R. S.; Jaeger, T. D.; Duncan, M. A.; Christie, R. A.; Jordan, K. D. *Science* **2004**, *304*, 1137–1140.
- (66) Elliott, B. M.; Relph, R. A.; Roscioli, J. R.; Bopp, J. C.; Gardenier, G. H.; Guasco, T. L.; Johnson, M. A. *J. Chem. Phys.* **2008**, *129*, 094303.
- (67) Robertson, W. H.; Diken, E. G.; Price, E. A.; Shin, J. W.; Johnson, M. A. *Science* **2003**, *299*, 1367–1372.
- (68) Miller, D. J.; Lisy, J. M. *J. Am. Chem. Soc.* **2008**, *130*, 15393–15404.
- (69) Carbacos, O. M.; Weinheimer, C. J.; Lisy, J. M.; Xantheas, S. S. *J. Chem. Phys.* **1999**, *110*, 5–8.
- (70) Bush, M. F.; Saykally, R. J.; Williams, E. R. *J. Am. Chem. Soc.* **2008**, *130*, 15482–15489.
- (71) O'Brien, J. T.; Williams, E. R. *J. Phys. Chem. A* **2008**, *112*, 5893–5901.
- (72) Sawamura, T.; Fujii, A.; Sato, S.; Ebata, T.; Mikami, N. *J. Phys. Chem.* **1996**, *100*, 8131–8138.
- (73) Mizuse, K.; Fujii, A.; Mikami, N. *J. Chem. Phys.* **2007**, *126*, 231101.
- (74) Walters, R. S.; Pillai, E. D.; Duncan, M. A. *J. Am. Chem. Soc.* **2005**, *127*, 16599–16610.
- (75) Carnegie, P. D.; Bandyopadhyay, B.; Duncan, M. A. *J. Phys. Chem. A* **2008**, *112*, 6237–6243.
- (76) Nicely, A. L.; Miller, D. J.; Lisy, J. M. *J. Am. Chem. Soc.* **2009**, *131*, 6314–6315.

However, the absence of bands attributable to a hydrated C-terminus in these spectra does not eliminate the possibility that some C-terminally hydrated isomers are present in the ion population, and computational results at the B3LYP/6-31++G** level of theory favor C-terminal hydration upon addition of the second water molecule.²⁷ More recent results from computational chemistry suggest that the binding energy of a single water molecule to the C-terminus and N-terminus is similar (within 1 kcal/mol) for protonated Val, Phe, Tyr, and Trp.⁸ For these and other ions with competitive hydration isomers, it can be challenging to assess isomer populations using IRPD spectra of isomer ensembles, even with the aid of theory, and ensemble average hydration thermodynamics measurements do not probe individual sites but are instead an average over all isomers present in the ion population. Relative energies from computational chemistry can also be highly dependent on the level of theory and basis set used, further complicating structural interpretation based on ensemble hydration energies and IRPD spectra alone.

Because ensemble average hydration energies often provide limited, indirect information about competition between individual hydration sites, a more direct, experimental probe of relative isomer populations is desirable. In principle, the relative contributions of hydration isomers that do not rapidly interconvert to an ion population can be determined from an IRPD spectrum if reference spectra for the isolated isomers are known. IRPD spectra can closely resemble linear absorption spectra, so that calculated absorption spectra of single isomers can in some cases be used as reference spectra. Alternatively, IRPD spectra of monoisomeric analogue complexes can be used as reference spectra.^{32,54} The accuracy of these approaches is difficult to assess, because there can be differences in spectral intensities and frequencies between IRPD spectra of analogue complexes and between IRPD and calculated linear absorption spectra. Elegant infrared hole-burning^{66,77} and IR/UV ion-dip^{59,64,78} spectroscopy experiments have yielded isomer-specific vibrational spectra of a variety of gas-phase ions, although experimental relative ion populations based on these isomer-specific spectra have not been reported. Here, we present the spectra of hydrated, protonated Phe and its derivatives to assign IRPD spectral bands unambiguously to various hydration isomers. IRPD kinetics at bands unique to the IRPD spectra of individual hydration isomers are probed to determine relative populations and energetics of hydration at each competitive hydration site for these ions. These are the first reported experimental relative binding energies of water to different binding sites of gas-phase ions.

Experimental Section

IRPD Spectroscopy. IRPD spectra of hydrated, protonated L-phenylalanine (Phe), N-methyl-L-phenylalanine (*N*-MePhe), *N,N*-dimethyl-L-phenylalanine (*N,N*-Me₂Phe), and L-phenylalanine methyl ester (PheOMe) are measured using a 2.75 T Fourier transform ion cyclotron resonance mass spectrometer along with a tunable OPO/OPA laser system.³² Phe and *N*-MePhe and the hydrochloride salts of *N,N*-Me₂Phe and PheOMe (Sigma-Aldrich, St. Louis, MO, U.S.A.) are prepared as 1 mM aqueous solutions. Borosilicate capillaries are pulled to an inner tip diameter of $\sim 1 \mu\text{m}$ and filled with the solution of interest. Electrospray is initiated by applying

an ~ 600 V potential relative to the heated metal capillary of the nanoelectrospray interface to a platinum filament in the filled capillary. Ions are directed through five stages of differential pumping into the cell of the instrument using electrostatic lenses. A copper block that surrounds the cell is cooled to 133 K for at least 8 h with a regulated flow of liquid nitrogen before all experiments.⁷⁹ An ~ 3.7 s pulse of dry nitrogen gas ($\sim 10^{-6}$ Torr) is used to improve ion trapping and thermalization, and this is followed by an ~ 7 s pumpdown to reduce the cell pressure to $<10^{-8}$ Torr. Precursor clusters are selected using stored waveform inverse Fourier transforms.

Mass-selected clusters are photodissociated using an OPO/OPA (LaserVision, Bellevue, WA, U.S.A.) pumped by the 1064 nm fundamental of a Nd:YAG laser (Continuum Surelight I-10, Santa Clara, CA, U.S.A.) at a 10 Hz repetition rate. Irradiation times between 5 and 60 s are used to produce substantial, but not complete, fragmentation of the isolated cluster. First-order photodissociation rate constants are determined from the precursor and product ion abundances after irradiation as a function of laser frequency and are corrected for frequency-dependent variations in laser power as well as BIRD, which occurs as a result of absorption of blackbody photons from the 133 K ion cell and cell jacket.

Computational Chemistry. A Monte Carlo conformational search for PheH⁺ with between 1 and 4 water molecules was performed with MacroModel 9.1 (Schrödinger, Inc., Portland, OR, U.S.A.) to generate at least 5000 geometries. Additional conformational searches for hydrated *N*-MePheH⁺, *N,N*-Me₂PheH⁺, and PheOMeH⁺ were performed after replacing hydrogen atoms in the initial PheH⁺ structures with methyl groups. Low-energy structures representing different isomers and water binding sites were selected for geometry optimization at the B3LYP/6-31G* level of theory in Q-Chem 3.1⁸⁰ (Q-Chem, Inc., Pittsburgh, PA, U.S.A.). Further optimization at the B3LYP/6-31+G** or MP2(full)/6-31+G** level of theory was done prior to calculating harmonic oscillator vibrational frequencies and intensities at the same level of theory. Additional single-point energy calculations were performed at B3LYP/6-311++G** or MP2/6-311++G** using the optimized B3LYP/6-31+G** geometries. Vibrational frequencies were scaled by 0.955 and convolved with a 100 and 15 cm⁻¹ fwhm Lorentzian for the 2900–3100 cm⁻¹ and 3100–3900 cm⁻¹ regions, respectively, to simulate experimental line widths. Zero-point energies, enthalpy, and entropy corrections at 0, 133, and 298 K were calculated using unscaled B3LYP/6-31+G** (respectively, MP2(full)/6-31+G**) harmonic oscillator vibrational frequencies.

Results and Discussion

Computational Results. Protonated Phe has four sites where a strong hydrogen bond to water can form: three hydrogen atoms at the protonated N-terminus and one hydrogen atom at the neutral C-terminus. Four low-energy conformers were identified for PheH⁺(H₂O) at the B3LYP/6-31+G** level of theory, all of which have a single favorable geometric framework, shown in Figure 1. In this geometry, one N-terminal hydrogen is close to the π -system of the phenyl ring, another N-terminal hydrogen is close to the carbonyl oxygen atom, and the phenyl ring and the carboxylic acid do not directly interact. This arrangement of the amino acid side chain, N-terminus, and C-terminus persists among all the low-energy structures identified at this level of theory for the hydrated ions investigated. This amino acid configuration is the same as that identified by Gao et al. for hydrated, protonated Phe and Tyr.⁸ However, new low-energy structures in which a water molecule interrupts the N-terminal hydrogen bond to the side chain π -system are

(77) Relph, R. A.; Guasco, T. L.; Elliott, B. M.; Kamrath, M. Z.; McCoy, A. B.; Steele, R. P.; Schofield, D. P.; Jordan, K. D.; Viggiano, A. A.; Ferguson, E. E.; Johnson, M. A. *Science* **2010**, *327*, 308–312.

(78) Sakota, K.; Kageura, Y.; Sekiya, H. *J. Chem. Phys.* **2008**, *129*, 054303.

(79) Wong, R. L.; Paech, K.; Williams, E. R. *Int. J. Mass Spectrom.* **2004**, *232*, 59–66.

(80) Shao, Y.; et al. *Phys. Chem. Chem. Phys.* **2006**, *8*, 3172–3191.

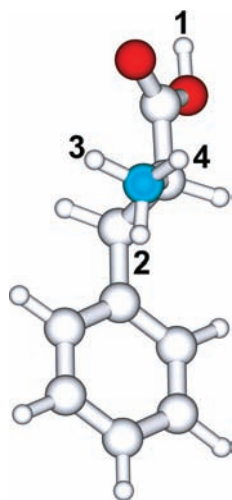


Figure 1. Schematic of amino acid geometry for B3LYP/6-31+G** low-energy structures calculated for PheH⁺ and its methylated derivatives. Acidic hydrogen atoms corresponding to the water binding sites at the carboxylic acid and N-terminal ammonium group are indicated with numbers.

identified, analogous to the **Trp1_C** structure described by Kamariotou, et al., for TrpH⁺(H₂O).⁸¹ The water molecule in these structures accepts a hydrogen bond from the N-terminus and donates a hydrogen bond to the π -system and has distinct spectroscopic properties due to the water- π hydrogen bond (vide infra). For the *N*-methyl derivatives of PheH⁺, structures in which a methyl group, rather than an N-terminal hydrogen atom, interacts with the π -system of the amino acid side chain were found to be at least 10–20 kJ/mol higher in Gibbs free energy at 133 K than the lowest-energy structure. Structures with water-water hydrogen bonding were also found to be energetically unfavorable for all of these ions by at least 15 kJ/mol, and no evidence of water-water hydrogen bonding was observed in the IRPD spectra of PheH⁺ with up to four water molecules (vide infra).

Calculated structures and relative B3LYP/6-31+G** Gibbs free energies at 0/133/298 K for PheH⁺(H₂O) and PheH⁺(H₂O)₄ are shown in Figures 2 and 3, respectively. Additional structures and energies for these and the other ions investigated are in the Supporting Information. In the following, we refer to the four acidic hydrogen sites by the numbering shown in Figure 1. Isomers are labeled according to the sites to which a water molecule or molecules are attached; e.g., in the **Phe2** isomer, the water molecule occupies site **2** (Figure 2) of PheH⁺(H₂O), and in **Phe1234**, water molecules occupy each of the four acidic hydrogen sites of PheH⁺(H₂O)₄ (Figure 3).

The relative energies of the low-energy structures of all of the ions investigated were found to depend on the basis set and level of theory. For PheH⁺(H₂O), **Phe4** is more stable than **Phe1**, **Phe2**, and **Phe3** by at least 1.6 kJ/mol with B3LYP/6-31+G**, whereas **Phe1** is more stable by at least 2.8 kJ/mol with B3LYP/6-311++G**//6-31+G**. MP2/6-311++G**//B3LYP/6-31+G** calculations favor **Phe2** by at least 1.1 kJ/mol. Even at 133 K, a small difference in the relative energy of an isomer in a thermal ion population can correspond to a large change in the population of that isomer. For instance, these B3LYP/6-311++G**//6-31+G** calculated energies correspond to a 133 K ion population that is ~90% **Phe1**, whereas for MP2/6-

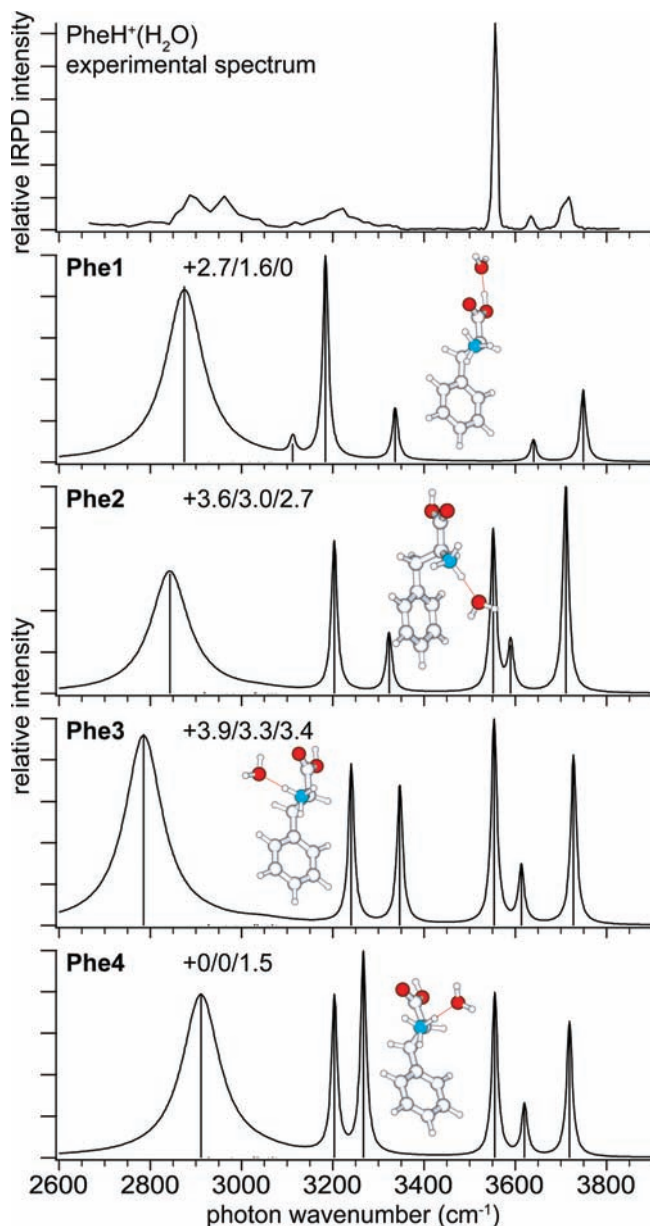


Figure 2. IRPD spectrum and low-energy structures and calculated spectra of PheH⁺(H₂O). Relative B3LYP/6-31+G** Gibbs free energies (kJ/mol) are reported at 0/133/298 K.

311++G**//B3LYP/6-31+G**, less than 1% of the ion population is **Phe1**. The range in relative energies in these calculations (Table 1) thus corresponds to a wide range of compositions of a thermal 133 K ion population, and no clear trend in relative energies among these four low-energy structures is predicted. Thus, determining relative water binding affinities for the four water binding sites in PheH⁺ based on levels of theory typically used for these types of ions^{8,33,59} cannot be done with confidence. Relative energies for isomers of all other ions investigated are included in the Supporting Information.

Comparisons of calculated absorption spectra of low-energy isomers can be useful in interpreting experimental IRPD spectra and determining which isomers likely contribute to the experimental ion population, but this proved difficult for many of these ions. Even for PheH⁺(H₂O)_{1,4}, where comparisons are more straightforward, there are still ambiguities. The IRPD spectrum of PheH⁺(H₂O)₁ (Figure 2) has a very intense band at 3557

(81) Kamariotou, A. Ph.D. Dissertation. École Polytechnique Fédérale de Lausanne, 2006.

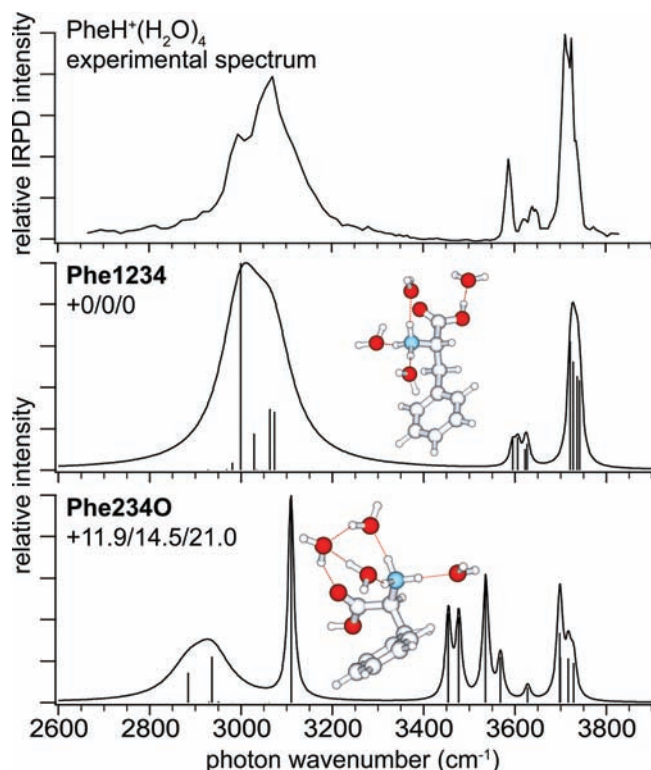


Figure 3. IRPD spectrum and low-energy structures and calculated spectra for $\text{PheH}^+(\text{H}_2\text{O})_4$. Relative B3LYP/6-31+G** Gibbs free energies (kJ/mol) are reported at 0/133/298 K.

cm^{-1} , closely matching the frequency of the carboxylic acid OH (COO–H) stretch calculated for structures **Phe2**, **Phe3**, and **Phe4**, at 3552, 3554, and 3555 cm^{-1} respectively. Thus, one or more of these structures contribute substantially to the experimental ion population. However, the relative intensity of the COO–H stretch band in the IRPD spectrum is significantly higher than those in the calculated spectra. The experimental band at 3634 cm^{-1} is matched in frequency most closely by the water OH symmetric stretch (s.s.) calculated for **Phe1** at 3640 cm^{-1} , and the water OH asymmetric stretch (a.s.) band predicted for **Phe1** at 3749 cm^{-1} overlaps with the broad experimental feature between 3697 and 3730 cm^{-1} , a range which includes the frequencies calculated for the water a.s. for **Phe2**, **Phe3**, and **Phe4**. Thus, based solely on a comparison of calculated spectra of low-energy isomers with the IRPD spectrum, it is difficult to assess whether a structure similar to **Phe1** is present in the ion population, in what proportion, and which of structures **Phe2**, **Phe3**, and **Phe4** contribute.

There are no bands indicative of water–water hydrogen bonding in the experimental spectrum of $\text{PheH}^+(\text{H}_2\text{O})_4$ (Figure 3, expected at $\sim 3450 \text{ cm}^{-1}$ for this ion), indicating that each of the four hydration sites is bound to a water molecule. This result is consistent with the lowest-energy calculated structure for $\text{PheH}^+(\text{H}_2\text{O})_4$ (**Phe1234**), which is 14.5 (30.9) kJ/mol lower in Gibbs free energy at 133 K at the B3LYP/6-31+G** (B3LYP/6-311++G**//6-31+G**) level of theory than the next-lowest-energy structure, in which water–water hydrogen bonding occurs (**Phe2340**). These structures are very similar to low-energy structures reported for $\text{PheH}^+(\text{H}_2\text{O})_4$ and $\text{TyrH}^+(\text{H}_2\text{O})_4$,⁸ $\text{TrpH}^+(\text{H}_2\text{O})_4$,^{8,81} and $\text{ValH}^+(\text{H}_2\text{O})_4$.²⁷ Although the calculated spectrum of **Phe1234** more closely resembles the measured spectrum, it does not reproduce the distinctive pattern of peaks observed between 3570 and 3650 cm^{-1} , indicating that the 133

K ion population is dominated by isomers that were not identified or that uncertainties in calculated harmonic frequencies and intensities are too great to provide detailed insight into the structural significance of the observed peak pattern.

IRPD Spectral Signatures for Water Molecules at Sites 1 and 2. To unambiguously assign the spectral bands for $\text{PheH}^+(\text{H}_2\text{O})_{1-4}$, IRPD spectra of hydrated, protonated phenylalanine derivatives between ~ 2650 and 3850 cm^{-1} were measured (Figure 4). Substituting methyl groups for one or more of the four water binding sites of PheH^+ reduces the number of available sites for direct water molecule attachment and also the number of possible conformers. For example, water can bind to the hydrogen atom at either the N- or C-terminus in N,N - Me_2PheH^+ , making it possible to readily assign the IRPD spectral bands for this ion. These assignments can be used to assign bands for hydrates of N - MePheH^+ and, in turn, PheOMeH^+ and PheH^+ .

The spectra of N,N - $\text{Me}_2\text{PheH}^+(\text{H}_2\text{O})_{1,2}$ are nearly identical in the higher-frequency region, except for a unique band at 3557 cm^{-1} for the singly hydrated species that is absent for the doubly hydrated species. There is no band at 3557 cm^{-1} in the spectra of $\text{PheOMeH}^+(\text{H}_2\text{O})_{1-3}$, N - $\text{MePheH}^+(\text{H}_2\text{O})_3$, and $\text{PheH}^+(\text{H}_2\text{O})_4$. PheOMeH^+ does not have a carboxylic acid group, and the number of attached water molecules is equal to the number of acidic hydrogen atoms in the other two ions. These results confirm that this band is the free COO–H stretch. The presence of this feature for N,N - $\text{Me}_2\text{PheH}^+(\text{H}_2\text{O})$, N - $\text{MePheH}^+(\text{H}_2\text{O})_{1,2}$, and $\text{PheH}^+(\text{H}_2\text{O})_{1-3}$, in which the number of acidic hydrogen atoms exceeds the number of water molecules, indicates that a substantial population of ions with no water molecules attached to the carboxylic acid group exists for these ions, in contrast to recent computational results, which suggest that site 1 is fully hydrated for $\text{PheH}^+(\text{H}_2\text{O})_{2,3}$.⁸ The very broad band between 2800 and 3200 cm^{-1} in each of these spectra is consistent with hydrogen bonded COO–H and NH stretch modes and gains in relative intensity with increasing hydration.

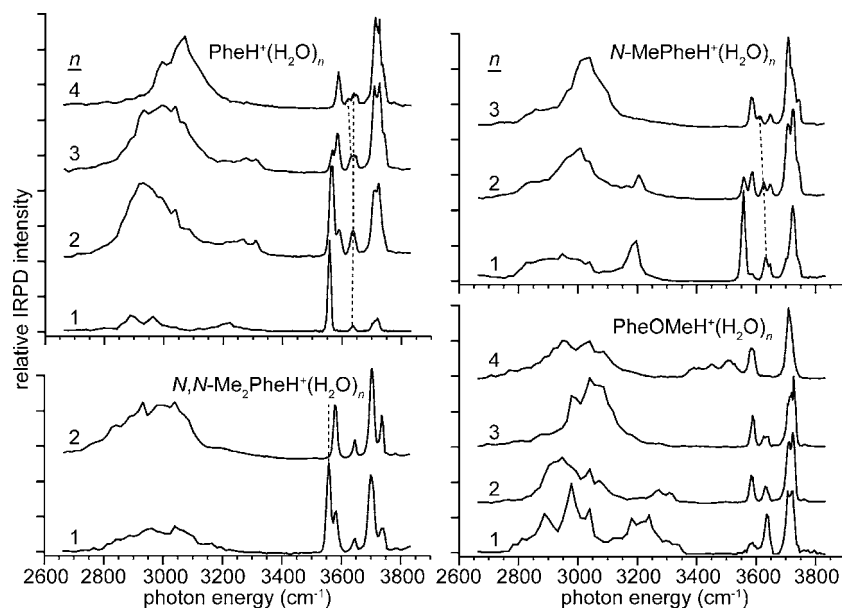
The IRPD spectra of N,N - $\text{Me}_2\text{PheH}^+(\text{H}_2\text{O})_{1,2}$ also contain four bands consistent with symmetric and asymmetric water OH stretches to the blue of the carboxylic acid stretch band. The lowest energy of these four bands (3580 cm^{-1}) is considerably red-shifted from the s.s. of a water molecule attached to ammonium (3610 cm^{-1}),⁸² although not to the extent that would indicate donation of a strong hydrogen bond by this water molecule, which should shift it below 3500 cm^{-1} . This is consistent with a water molecule attached to site 2 that is stabilized by donating a weak hydrogen bond to the π -system of the phenylalanine side chain, indicating the methyl groups are at sites 3 and 4. A similar red-shift for a water s.s. has been observed for $\text{TrpH}^+(\text{H}_2\text{O})$, where it was assigned to a water molecule bound between the protonated N-terminus and the π -system of the Trp side chain.⁸¹ A band at this frequency is also observed for N - $\text{MePheH}^+(\text{H}_2\text{O})_{1-3}$, $\text{PheOMeH}^+(\text{H}_2\text{O})_{1-3}$, and $\text{PheH}^+(\text{H}_2\text{O})_{2-4}$, indicating that structures with a similar π -bound water molecule at site 2 are present for these ions. Interestingly, no strong feature is observed at this frequency for $\text{PheH}^+(\text{H}_2\text{O})$, which suggests that such a structure is not present in significant abundance for this ion and that methylation of the N-terminus or carboxylic acid group makes site 2 more competitive for attachment of the first water molecule.

The other water OH s.s. of N,N - $\text{Me}_2\text{PheH}^+(\text{H}_2\text{O})_{1,2}$ (3646 cm^{-1}) is very close to that of a neutral water molecule (3657

(82) Pankewitz, T.; Lagutschenkov, A.; Niedner-Schatteburg, G.; Xantheas, S. S.; Lee, Y. T. *J. Chem. Phys.* **2007**, *126*, 074307.

Table 1. Relative Calculated Energies for Structure of PheH⁺(H₂O) at 0/133/298 K in kJ/mol

	Phe1	Phe2	Phe3	Phe4
B3LYP/6-31+G**	+2.7/1.6/0	+3.6/3.0/2.7	+3.9/3.3/3.4	+0/0/1.5
B3LYP/6-311++G**// 6-31+G**	+3.8/0/0	+3.7/3.9/1.7	+4.0/6.3/2.4	+0/2.8/1.5
MP2/6-31+G**// B3LYP/6-31+G**	+11.5/8.3/6.2	+1.4/0/0	+7.2/6.2/7.9	+0/1.1/1.2
MP2(full)/6-31+G**	+10.7/10.4/9.3	0/0/0	+2.9/2.7/2.6	+2.7/1.8/0.3

**Figure 4.** IRPD spectra of hydrated, protonated Phe; *N*-MePhe; *N,N*-Me₂Phe; and PheOMe at 133 K.

cm⁻¹) and is consistent with a water molecule attached to site **1**, which carries no formal charge and causes little red-shifting of the water s.s. band. There is no band at this frequency for PheOMeH⁺(H₂O)₁₋₃ (the band at 3630 cm⁻¹ corresponds to a water molecule at site **4**), further confirming this assignment. The a.s. frequencies associated with water molecules at sites **1** and **2** can be determined by noting that the a.s. band at 3735 cm⁻¹ in the spectra of *N,N*-Me₂PheH⁺(H₂O)_{1,2} is absent for PheOMeH⁺(H₂O)₁₋₃, whereas strong bands near 3697 cm⁻¹ are present for all of these species. Thus the 3735 cm⁻¹ band is assigned to the a.s. of a water molecule at site **1** and the 3697 cm⁻¹ band, to the a.s. of the π -bound water molecule at site **2**.

IRPD Spectral Signatures for Water Molecules at Sites 3 and 4. Because bands corresponding to water–water hydrogen bonding are not observed for any of the ions except PheOMeH⁺(H₂O)₄, where these occur between ~3350 and 3550 cm⁻¹, all bands between 3580 cm⁻¹ and 3735 cm⁻¹ not assigned to the above two types of water molecule must correspond to water molecules attached to sites **3** and/or **4**. In the spectra of *N*-MePheH⁺(H₂O)₁₋₃, an additional water OH s.s. feature appears at ~3626 cm⁻¹ for the singly and doubly hydrated ion that abruptly red-shifts to 3610 cm⁻¹ for the triply hydrated species. Likewise, for PheH⁺(H₂O)₁₋₄, a new water OH s.s. band appears at 3620 cm⁻¹ for the fully hydrated species that replaces a higher-frequency band at 3630 cm⁻¹ for PheH⁺(H₂O)₁₋₃. The similar frequencies of these 3626/3620 cm⁻¹ bands for *N*-MePheH⁺(H₂O)_{1,2}/PheH⁺(H₂O)₄ suggest that they correspond to water molecules bound to the same type of hydration site. The s.s. band of a water molecule in a fourth type of binding geometry appears in the spectra of PheH⁺(H₂O)_{3,4} at 3639 cm⁻¹. This band overlaps considerably with the 3646 cm⁻¹ band for these ions, and it is not clear to what extent it is present for PheH⁺(H₂O)_{1,2}, where the s.s. feature in this region is weak.

Because all acidic hydrogen atoms are hydrated in PheH⁺(H₂O)₄, the difference in s.s. frequency between the water molecules associated with the 3620 and 3639 cm⁻¹ bands for this ion can be attributed to a slight, but significant, difference in the strength of their interaction with the *N*-terminus or the nearby carbonyl oxygen atom. Indeed, B3LYP/6-31+G** calculations predict that the water molecules bound at these two sites are located at different distances from the carbonyl oxygen atom, with the nearest hydrogen atom of the site **3** water molecule ~0.5 Å closer (H-bond distance 2.2 Å) than that of the site **4** water molecule. This results in a calculated red shift of ~30 cm⁻¹ for the site **3** water molecule relative to **4**, in satisfactory agreement with the experimental value of 19 cm⁻¹, whereas calculations indicate that the **Phe3** water molecule s.s. band should nearly coincide with the s.s. band of **Phe2** (Figure 2). Thus, the 3626/3620 cm⁻¹ bands for *N*-MePheH⁺(H₂O)_{1,2}/PheH⁺(H₂O)₄ are attributed to water molecules at site **3**, and the 3639 cm⁻¹ band is attributed to a water molecule at site **4**. The discrepancy in the experimental and calculated red shifts for these bands may be due to anharmonicity of the OH stretches that is not accounted for in the calculated harmonic frequencies or to minor differences between calculated structures and the structure present in the experimental ion population, such as a 180° rotation of the C-terminus about the C'–C^α axis.

Because the other water OH s.s. features for *N*-MePheH⁺(H₂O)₁₋₃ and PheH⁺(H₂O)₁₋₃ do not shift substantially with increasing hydration state, the red shifts observed for the s.s. of the water molecule at site **3** with increasing hydration suggest that a small, localized change in the binding geometry of the water molecule at site **3** occurs without disrupting the hydrogen bond donated by the bridging water molecule at site **2**. One possibility, consistent with calculated structures (see Supporting Information), is that the optimal

torsion angle of the N-terminus with respect to the amino acid backbone for binding a water molecule at site **3** is different from that for the π -bound water molecule at site **2**, leading to frustration of the site **3** water molecule when both sites are hydrated and a corresponding frequency shift for this mode. Because the frequency shift for this mode is not observed until the third water molecule is added to the ion, these results suggest that binding a water molecule to either site **2** or **3** hinders binding an additional water molecule to the other site, whereas binding a water molecule to site **1** (the distant carboxylic acid hydrogen atom) does not.

Additional strong, often broad, bands occur below 3400 cm^{-1} in all of these spectra that support the above analysis but are less useful for detailed structural determination. Bands between 3150 and 3350 cm^{-1} occur for all of the ions investigated when the number of acidic hydrogen atoms exceeds the number of attached water molecules. These bands are much too low in energy to be assigned a free COO–H stretch and are instead consistent with free NH stretch modes, in agreement with IRPD spectra of other hydrated, protonated Val²⁷ and Trp.⁸¹ Bands below 3100 cm^{-1} in these spectra are associated with amino acid backbone and side chain CH stretch modes, which are typically very weak in IRPD spectra, and hydrogen-bonded COO–H and NH stretch modes, which can often be very intense and broad. In general, the broad feature in this region gains substantially in relative intensity with increasing hydration state for a given ion, indicating that the feature is predominantly attributed to water-bound COO–H and NH stretches. The shape of this feature changes little for N,N -Me₂PheH⁺(H₂O)_{1,2}, consistent with significant populations of both C-terminally and N-terminally hydrated isomers for the singly hydrated species. For the other ions investigated, this feature blue shifts with increasing hydration state, consistent with less charge transfer from the protonated N-terminus to attached water molecules as additional water molecules are added. There does appear to be some structure to this feature for some of the ions investigated, but the poor resolution of these subbands makes more detailed assignments challenging.

Isomer Populations from Photodissociation Kinetics. In principle, the relative populations of the two different isomers of N,N -Me₂PheH⁺(H₂O) (water attached to either site **1** or **2**) that contribute to the measured IRPD spectrum could be obtained from a linear superposition of the spectra of the individual species, if the spectrum for each species was accurately known. Calculated relative intensities do not always correspond closely to relative IRPD intensities, and IRPD spectral intensities may not reflect linear absorption intensities,^{54,71,83} making it difficult to obtain meaningful quantitative data from comparisons of measured to calculated spectra. However, if the ion isomers do not interconvert rapidly on the time scale of the experiment and each has a unique spectrum, then the contributions of each isomer can be obtained from dissociation kinetic data at wavelengths unique to each isomer. Kinetic data for N,N -Me₂PheH⁺(H₂O) measured at three different frequencies are shown in Figure 5. This ion does not dissociate measurably at 133 K due to BIRD on the time scale of these experiments (120 s). The photodissociation kinetics are clearly biexponential at each of these wavelengths. To confirm that the biexponential data are due to two isomers with different absorption cross sections and not due to an artifact of partial overlap of the ion

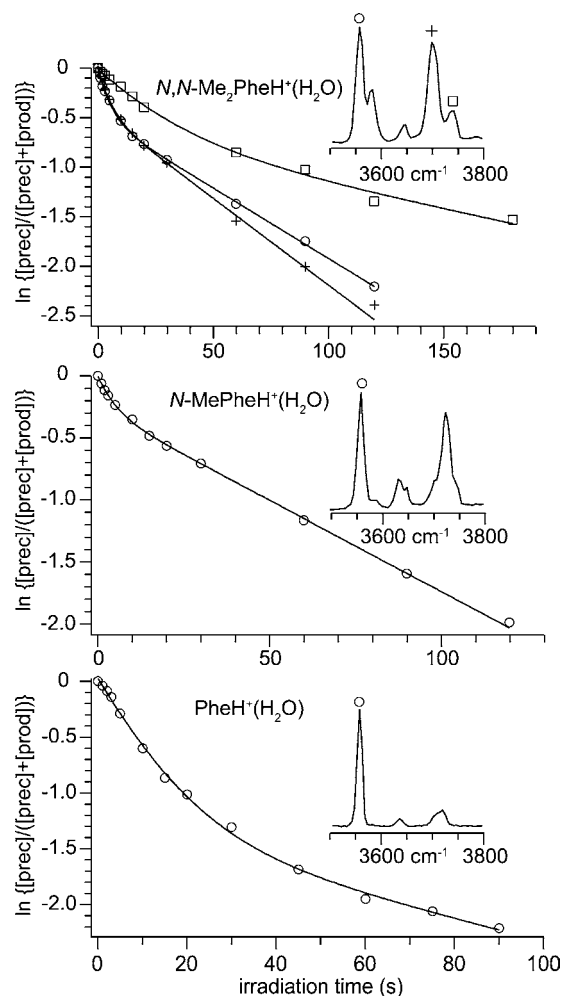


Figure 5. Laser photodissociation kinetics at 133 K for N,N -Me₂PheH⁺(H₂O), N -MePheH⁺(H₂O), and PheH⁺(H₂O) at laser frequencies 3557 (○), 3697 (+), and 3740 cm⁻¹ (□), with partial IRPD spectra inset (see Figure 4). Lines represent a least-squares biexponential fit to the data. Note that the y-axis is logarithmic to make clear the biexponential kinetic behavior.

cloud with the laser beam, photodissociation kinetics of N,N -Me₂PheH⁺(H₂O)₃ at 3715 cm⁻¹ (water OH a.s.) were measured. These data are monoexponential to greater than 95% depletion of the precursor ion population, consistent with previous measurements of other extensively hydrated ions measured with this apparatus.^{71,84}

The isomer with the water molecule at site **2** has a free COO–H stretch band at 3557 cm^{-1} and a water OH a.s. band at 3697 cm^{-1} , whereas the isomer with the water bound to site **1** does not have a free carboxylic acid OH band and its water OH a.s. band is at 3740 cm^{-1} . The former structure is depleted rapidly by the on-resonance radiation at both 3557 and 3697 cm^{-1} , whereas the latter structure dissociates more slowly due to off-resonant absorption or slow interconversion to the resonant isomer. A biexponential fit to the 3557 cm^{-1} data yields a relative population of 39% associated with the water molecule at site **2** (0.197 s^{-1}) and 61% for the water molecule at site **1** (0.014 s^{-1}). The 3697 cm^{-1} data yield nearly identical results: a 35% relative population of the resonant (site-2-bound) isomer (0.193 s^{-1}), and 65% for the nonresonant isomer (0.017 s^{-1}).

(83) Kupser, P.; Steill, J. D.; Oomens, J.; Meijer, G.; von Helden, G. *Phys. Chem. Chem. Phys.* **2008**, *10*, 6862–6866.

(84) Prell, J. S.; O'Brien, J. T.; Williams, E. R. *J. Am. Soc. Mass Spectrom.* **2010**, *21*, 800–809.

Table 2. Relative Conformer Populations for *N,N*-Me₂PheH⁺(H₂O), *N*-MePheH⁺(H₂O), and PheH⁺(H₂O) at 133 K Based on Biexponential Fits to 3557 cm⁻¹ Photodissociation Data

water binding site	1	2	3	4
<i>N,N</i> -Me ₂ PheH ⁺ (H ₂ O)	65 ± 4%	35 ± 4%	N/A	N/A
<i>N</i> -MePheH ⁺ (H ₂ O)	77%	← 23% →		N/A
PheH ⁺ (H ₂ O)	26%		← 74% →	

Results for the weaker band at 3740 cm⁻¹ yield slightly different populations (49% for the site-1-bound isomer), but some population of the nonresonant, site-2-bound isomer likely absorbs at this frequency due to the high-energy tail of its much stronger OH a.s. band centered at 3697 cm⁻¹, which is apparent in the experimental spectrum (Figure 5). These results indicate that ~35 ± 4% of the *N,N*-Me₂PheH⁺(H₂O) ion population has a site-2-bound water molecule and ~65 ± 4% at site 1.

Similar experiments probing the free COO–H stretch at 3557 cm⁻¹ (Figure 5) for *N*-MePheH⁺(H₂O) indicate an ~23% population with the water molecule at sites 2 or 3 (0.086 s⁻¹) and an ~77% population with the water molecule at site 1 (0.010 s⁻¹). Probing this band for PheH⁺(H₂O) indicates a 74% population for site 2, 3, or 4 (0.209 s⁻¹) and a 26% population for site 1 (0.015 s⁻¹). These results for PheH⁺(H₂O), *N*-MePheH⁺(H₂O), and *N,N*-Me₂PheH⁺(H₂O), which are summarized in Table 2, are the first reported determinations of isomer populations from IRPD kinetic data. The substantially greater population of N-terminally bound water molecules for PheH⁺(H₂O) in comparison to the other two ions indicates that the N-terminus is a much more favorable site without methylation and that site 4 is the most favorable hydration site in PheH⁺(H₂O). The similarly large population of site-1-bound isomers for *N*-MePheH⁺(H₂O) and *N,N*-Me₂PheH⁺(H₂O) indicates that attachment of the water molecule to this site is greatly preferred over attachment to site 2 or 3. An equal preference for sites 2 and 3 in *N*-MePheH⁺(H₂O) would result in a site-1-bound population fraction for *N*-MePheH⁺(H₂O) that is exactly half that for *N,N*-Me₂PheH⁺(H₂O). Instead, the fraction of site-1-bound isomers is nearly the same for both ions; thus, site 2 must be more favorable than site 3. In summary, the kinetics of these ions indicate that the four water binding sites in PheH⁺(H₂O) are ordered as follows in terms of decreasing affinity for the water molecule: 4 > 1 > 2 > 3. This same ordering applies to the available hydration sites in *N*-MePheH⁺(H₂O) and *N,N*-Me₂PheH⁺(H₂O). These results are consistent with crude relative ion population estimates based on peak heights and integrated peak areas for the experimental IRPD spectra of these ions and their higher hydrates. Somewhat ironically, this is the same order obtained from the computationally least expensive calculations (B3LYP/6-31+G**) but not from the MP2 calculations or those with a larger basis set (6-311++G**).

The slower rate constants in the biexponential photodissociation kinetics correspond either to dissociation of a water molecule from the nonresonant isomer or to interconversion of the nonresonant and resonant isomers. Thus, the longer lifetime is a lower bound for the interconversion lifetime between isomers. For *N,N*-Me₂PheH⁺(H₂O), the lifetime for moving the water molecule from site 1 to site 2 must be >71 s at 133 K. This long equilibration lifetime indicates a high barrier for interconversion, which is consistent with the ~180° rotation of the water molecule and passage around a bulky methyl group necessary for interconversion between these two isomers. A lower limit of ~36 kJ/mol for the 133 K Gibbs free energy barrier to move a water molecule from site 1 to 2 can be

determined using this lifetime and the Eyring equation. Interestingly, interconversion between structures with carboxylic acid hydrogen-bound and NH-bound water molecules for PheH⁺(H₂O) may have an even longer lifetime (at least ~98 s), indicating that detachment from the N- or C-terminus and rotation of the water molecule, i.e., not simply passage around the N-terminal methyl groups, contribute substantially to the interconversion barrier for both this ion and *N,N*-Me₂PheH⁺(H₂O). Because these lifetimes are so long, these isomers could potentially be kinetically trapped in a supersonic expansion if they are not allowed substantial equilibration time after formation. Differences in these kinetics with varying ion equilibration times on the order of hundreds of seconds before laser irradiation could confirm whether kinetic trapping has occurred in such instances.

Relative Water Affinities from Isomer Populations. For a thermal population of ions at a temperature *T*, the difference in Gibbs free energy, Δ*G*_{*T*}(*m* – *n*), between nondegenerate isomers *m* and *n* is related to their relative population sizes *p*_{*m*} and *p*_{*n*} by the equation Δ*G*_{*T*}(*m* – *n*) = –*k*_B*T* ln(*p*_{*m*}/*p*_{*n*}), where *k*_B is Boltzmann's constant. Thus, the relative binding energies to sites 1, 2, 3, and 4 for these ions can be obtained from the measured relative populations (Table 2). For *N,N*-Me₂PheH⁺(H₂O), binding a water molecule is more favorable at site 1 than at site 2 by 0.7 ± 0.2 kJ/mol at 133 K.

Upper and lower bounds for the energy difference between isomers with water molecules at sites 1 and 2 in *N*-MePheH⁺(H₂O) can be obtained by first noting that site 3 is the least favorable of these sites for water attachment. Thus, in the limit that no ion population has the water molecule attached to site 3, the populations at sites 1 and 2 are 77% and 23%, respectively. This corresponds to a lower bound of 1.3 kJ/mol for the energy difference between site-1- and site-2-bound isomers. In the opposite limit where sites 2 and 3 are equally favorable, 1/2 × 23% = 11.5% of the ion population is associated with each of these two sites, and 77% with site 1, corresponding to an energy difference of 2.1 kJ/mol between site 2/3 and site 1. The smaller fraction of site-1-bound isomers in *N,N*-Me₂PheH⁺(H₂O) relative to *N*-MePheH⁺(H₂O) indicates that solvation of the N-terminal charge by the carbonyl oxygen atom in *N*-MePheH⁺(H₂O) that does not occur for *N,N*-Me₂PheH⁺(H₂O) makes the N-terminus a less attractive hydration site despite the somewhat lower gas-phase basicity of *N*-MePheH⁺.

A lower bound for the difference in energy between site-4- and site-1-bound isomers of PheH⁺(H₂O) can also be obtained from the relative populations in Table 2 in combination with the above thermodynamic information. The substantially higher fraction of N-terminally bound water molecules for PheH⁺(H₂O) indicates that site 4 is the major water binding site. Thus, in the limit that site 2 is just 1.3 kJ/mol less favorable than site 1 for PheH⁺(H₂O), the total population fraction at sites 2 and/or 3 should be (23/77) × 26% = 8%. The remainder, (74% – 8%) = 66%, of N-terminally bound isomers must have the water molecule at site 4. This corresponds to a ≥ 1.0 kJ/mol preference for site 4 over site 1 in PheH⁺(H₂O). An upper bound is obtained by assuming instead that all 74% of the N-terminally bound isomers have a water molecule at site 4, corresponding to a preference of 1.2 kJ/mol over site 1. These results, summarized in Table 3, are the first reported relative energies of ion isomers derived entirely from IRPD kinetics. The uncertainties in these values are significantly lower than those from calculations at

Table 3. Relative Energies (kJ/mol) of Conformers of N,N -Me₂PheH⁺(H₂O), N -MePheH⁺(H₂O), and PheH⁺(H₂O) at 133 K Based on Experimental Conformer Populations

water binding site	1	2	3	4
N,N -Me ₂ PheH ⁺ (H ₂ O)	0	+0.7 ± 0.2	N/A	N/A
N -MePheH ⁺ (H ₂ O)	0	+1.3–2.1	>+2.1	N/A
PheH ⁺ (H ₂ O)	+1.0–1.2	>+2.3	>+2.3	0

levels of theory typically used for systems of this size, and these experimental values should provide a stringent benchmark for theory.

Conclusions

The sites of water binding to protonated Phe with up to four water molecules and the relative binding energies of these closely competitive sites can be obtained from IRPD spectroscopy and photodissociation kinetics of this ion and its protonated, methyl-substituted derivatives, which make it possible to systematically assign bands in congested spectra where multiple hydration isomers contribute substantially to the ion population. The population of each isomer can be obtained by fitting the kinetic data measured at unique frequencies at which each isomer absorbs, and the relative Gibbs free energies of the isomers are obtained from these populations. Results clearly show that one specific hydrogen atom at the N-terminus of PheH⁺ is the preferred water binding site at 133 K, followed by the carboxylic acid hydrogen, an N-terminal hydrogen where the attached water molecule donates a hydrogen bond to the side chain π -system, and finally the remaining N-terminal hydrogen atom. For N,N -Me₂PheH⁺(H₂O), the carboxylic acid bound isomer is 0.7 ± 0.2 kJ/mol more stable than the competing N-terminally bound structure. This value increases

slightly (to 1.3–2.1 kJ/mol) for N -MePheH⁺(H₂O) due to the partial solvation of the N-terminal charge by the carbonyl oxygen atom. For PheH⁺(H₂O), the most favorable N-terminal water-binding site is 1.0–1.2 kJ/mol more favorable than the carboxylic acid site. The relative binding energies of water to various sites in these molecules are obtained entirely from experimental data, and these results are not consistently predicted by either hybrid density functional theory or MP2 calculations at levels typically used for systems of this size. These IRPD methods can be especially useful when calculations do not yield consistent thermochemical values or when calculated absorption spectra do not sufficiently reproduce the experimentally measured spectra.

More detailed thermochemical data could be obtained by measuring the dissociation kinetics as a function of temperature to determine the relative enthalpies and entropies of the different isomers. These results, in combination with techniques that measure ensemble average binding energies, such as high pressure mass spectrometry or blackbody infrared radiative dissociation, can be used to obtain isomer-specific absolute binding energies. This IRPD kinetic method has the advantage over conventional two-laser “hole-burning” experiments in that only a single laser is required, but this method is only applicable when interconversion barriers between isomers are high.

Acknowledgment. The authors thank Daniel J. Kennedy for help with data acquisition and the National Science Foundation (Grant CHE-0718790) for generous financial support.

Supporting Information Available: Full citation for ref 80 and all calculated structures, energies, and spectra. This material is available free of charge via the Internet at <http://pubs.acs.org>.

JA102765W